

A RELIC SAND WAVE FIELD IN A TIDAL CHANNEL

Shelley J. Whitmeyer¹, Duncan FitzGerald²

1. Boston University, Dept. of Earth Sciences, 685 Commonwealth Ave., Boston, MA, 02215, USA, shelleyj@bu.edu.
2. Boston University, Dept. of Earth Sciences, 685 Commonwealth Ave., Boston, MA, 02215, USA, dunc@bu.edu.

Abstract: A sand wave field in the eastern flood channel of Moriches Inlet was monitored for eight weeks during the summer of 2005. Bathymetric data show sand waves which are 15 m long and 39 cm tall with shallow slip faces. These sand waves remained stationary over the eight week study. Analysis based on work by van Rijn (1984) and Yalin (1964) suggests that these sand waves were created when the current velocity reaches 80 cm/s. However, the peak current speeds recorded during this study are less than 60 cm/s. Infrequent, high-energy events are believed to have created these sand waves. A hypothetical event creating these sand waves is described based on a linear analysis of tidal range and peak tidal currents. Water level data from Sandy Hook, NJ and Shinnecock Inlet, NY are used to identify this event. This study demonstrates that episodic events may control sand wave morphology and that once emplaced the sand waves become autonomous.

INTRODUCTION

Sand waves are potential hazards in navigation channels. As they develop within the channel or migrate into the channel from adjacent areas, they reduce the project depth. In the Panama City Entrance Channel and in the Columbia River sand waves reduce the navigation depth by half. In addition to causing channel shoaling, sand waves also decrease the depth-averaged flow velocity and increase turbulence. To efficiently manage tidal navigation channels and model sediment transport it is necessary to understand and predict the geometry, distribution, and migration rates of sand waves.

The conditions under which sand waves develop have been well defined through flume experiments. Under these controlled conditions variations in grain size, water depth, and flow velocity create predictable changes in bedform morphology. However, these

predictive relationships are less reliable to natural settings, especially in tidal channels. Complications arise because:

1. water depth, flow velocity, and grain size are not independent of one another,
2. channel morphology and flow conditions typically are not in equilibrium,
3. sand supply may be limited, and
4. wave-current interaction may change flow conditions.

Moriches Inlet, which is located along the South Shore of Long Island, New York, USA, is a wave-dominated, micro-tidal inlet (Figure 1). It is a sand rich-inlet that connects Moriches Bay directly to the Atlantic Ocean. The focus of this study is the sand wave field in the eastern flood channel (2-4 m) of Moriches Bay. The sand wave field is on a shallow bank (~2-3 m deep) between two relatively deep channels; the west is ebb dominated and the east is flood dominated. Data collected at the inlet include eight weekly bathymetric surveys, sediment samples ($d_{50}=0.43$ mm), current measurements (peak tidal currents 60 cm/s), and water level data (spring range=1 m, neap range=60 cm). The field study was designed to measure the geometry of the sand waves, document any morphological change, track sand wave migration, and record the hydraulic conditions.

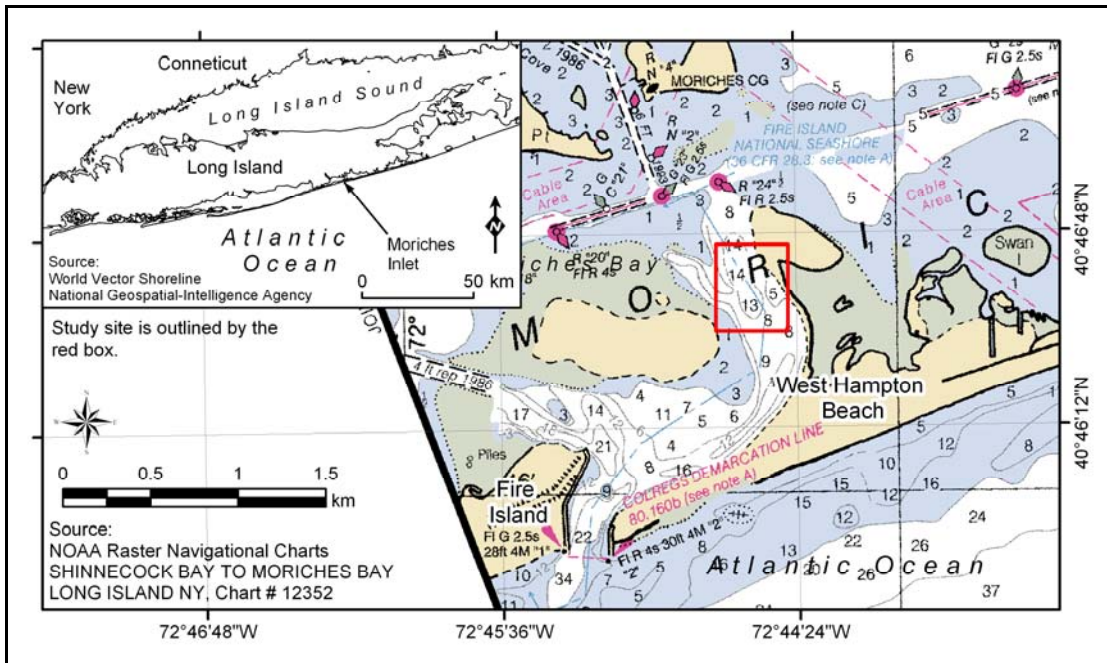


Figure 1. Location of the study area within Moriches Bay. Study site is delineated by the red box.

SAND WAVE MOPHOLOGY

Weekly bathymetric surveys were collected using an Innerspace Model 455 single-beam depth sounder (200 kHz and 8°). The location of the boat was tracked with a Trimble AgGPS 132 GPS (sub-meter accuracy). Two surveys were taken over the first 24 hours to capture sand wave response to a spring tide. Thereafter, the surveys were collected

weekly (29 July, 5 August, 12 August, 19 August, 26 August, and 2 September). Sand waves in this area can generally be divided into two groups- well-defined, flood-orientated sand waves on the bank and smaller, ebb-orientated sand waves in the ebb channel.

Bathymetric surfaces were modeled using ArcGIS™. A Triangulated Irregular Network (TIN) was created from the individual soundings for each survey. The TINs were converted to grids in order to run more efficiently in ArcMap™ (Figure 2). The error of the bathymetric interpolation is ± 12 cm. The sand wave location, height, wavelength, and orientation were identified on each of the eight surveys. Cross-sectional profiles were extracted from the bathymetric grid along each of the survey lines running northwest-southeast and then imported into MatLab for analysis with a script written by the author. The crests and troughs of the sand waves were identified by calculating the approximate derivative of each cross section (Figure 3). The wavelength, height, and slope of the sand waves calculated from the crests and troughs. This information was then imported back into ArcMap™. In ArcMap™, the sand wave crests were delineated along those crest points imported from MatLab.

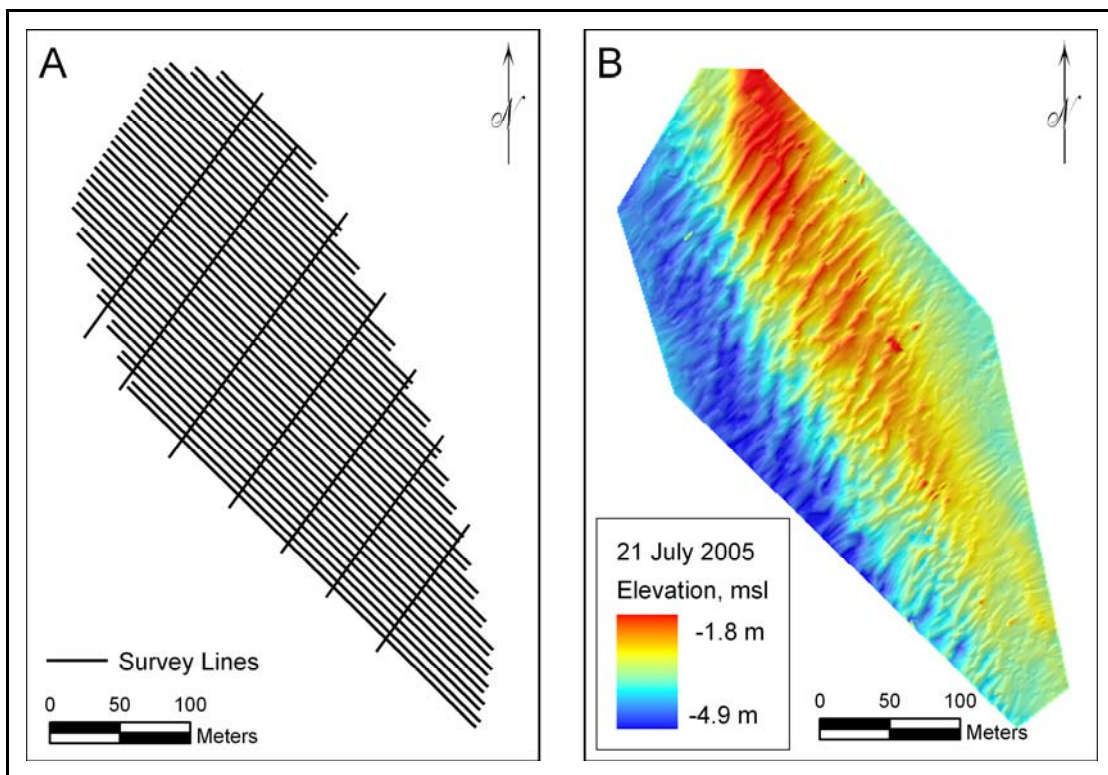


Figure 2. a) Survey track lines along which bathymetric data were collected. b) Bathymetric map of the study area on 21 July 2005. The map is a one meter grid.

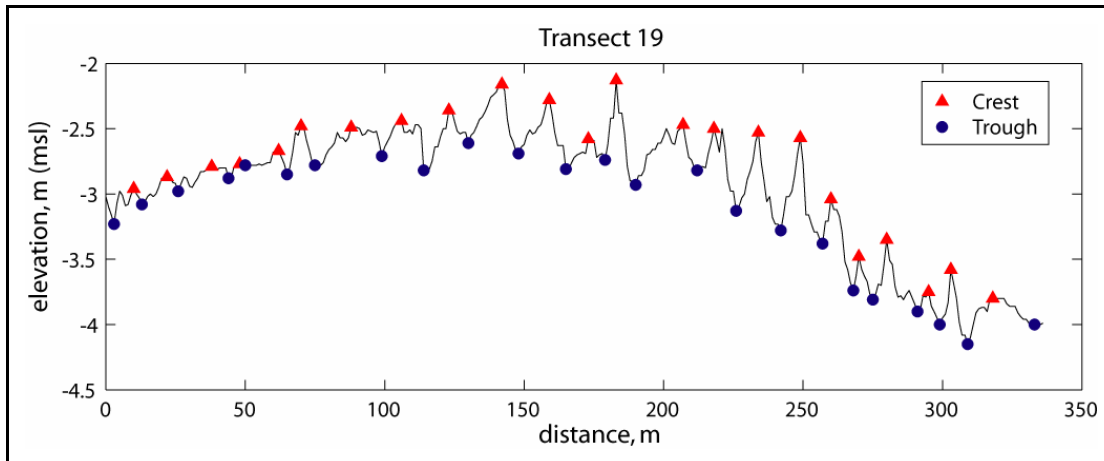


Figure 3. Cross Section from transect 19 which runs through the center of the study area. Crests are shown as triangles and the troughs are shown as circles.

Bathymetric surveys within the 0.07 km^2 study area show two unique morphologies. There are larger, better-defined flood-dominant sand waves on the shallow bank, and smaller ebb-dominant sand waves in the ebb channel. The mean height was 39 cm and the wave length was 15 m over the entire study area. The average spacing of the ebb- and flood-orientated sand waves was the same, but their heights varied. The ebb-orientated sand wave height was 23 cm compared to the larger flood-orientated sand wave height which was 46 cm. The slip face slopes are shallow. The slopes are sub-horizontal, varying from 3.6° to 4.4° . There was little variation in these dimensions during the study period. Morphological changes between the spring and neap tide cycles were not documented.

The location of the sand wave crests were tracked over the seven week study period (Figure 4). Considering the horizontal uncertainty of the depth soundings ($\pm 1 \text{ m}$), an uncertainty of $\pm 2 \text{ m}$ should be assumed when comparing surveys. These data indicate a lack of systematic migration of the sand waves over the study period. Realignment, flexing, and some bifurcation of the crests occurred. However, bifurcating crests usually returned to their previous continuous configuration, and therefore, may be the result of variations in interpolation due to differences in the location of the soundings between surveys rather than changes in the morphology.

PREDICTED SAND WAVE HEIGHT

Laboratory studies (Southard 1971; Southard, et al. 1990) and field studies (Aliotta, et al. 1987; Boothroyd, et al. 1975; Dalrymple, et al. 1978; Dalrymple, et al. 1995; Gabel 1993; Mazumder 2003; McCave 1971; Yalin 1964; Zarillo 1982) have demonstrated that bedform morphology is a function of flow depth, grain size, and flow velocity or shear stress. Yalin (1964) and van Rijn (1984) have estimated the dimensions (height and spacing) of sand waves based on the shear stress. Yalin's derivation for sand wave spacing begins with non-dimensional parameters for the "relative roughness" and "grain-size Reynolds number," i.e., the particle Reynolds number. The Reynolds number

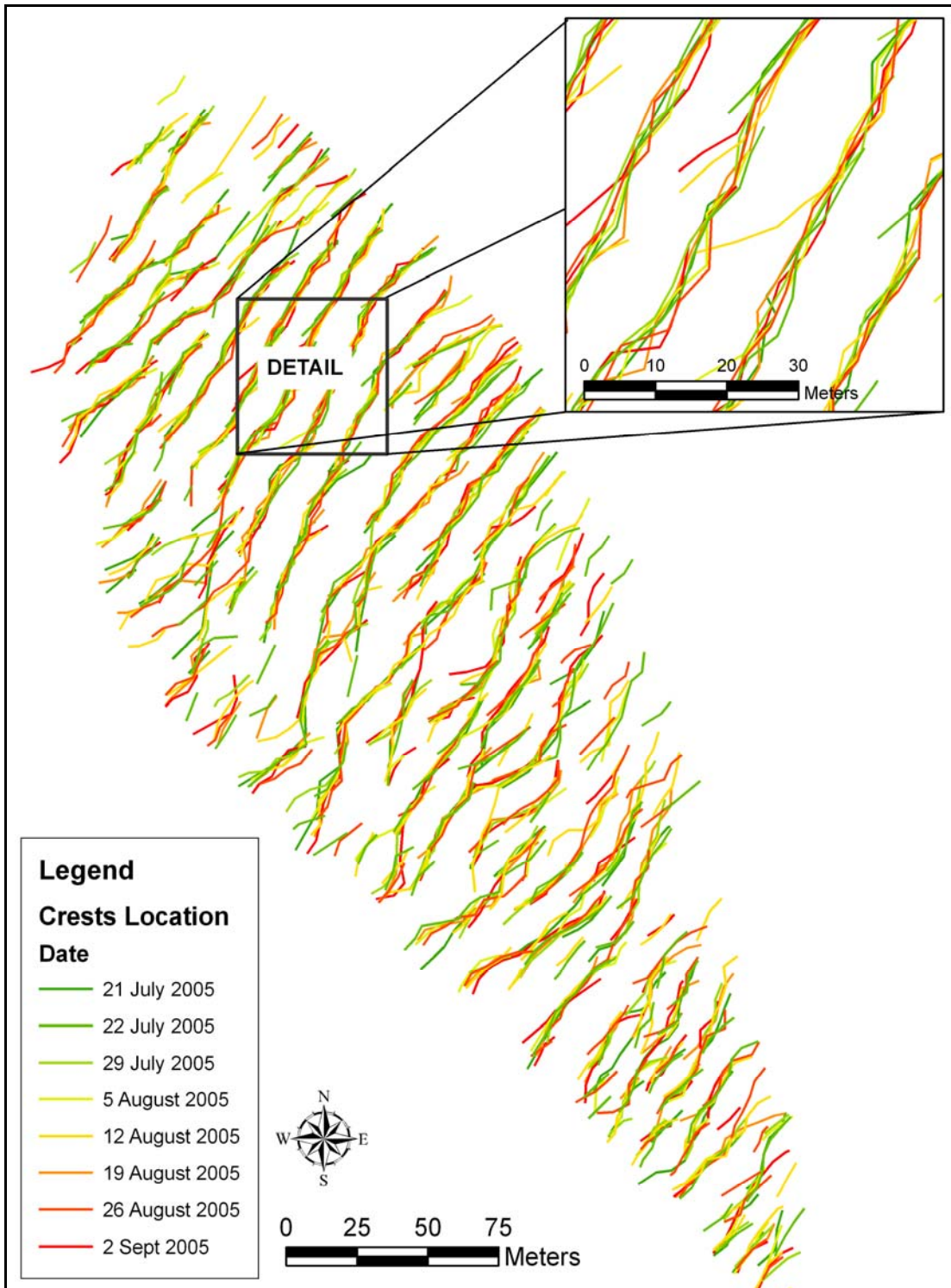


Figure 4. Lines show location of sand wave crests from 21 July to 2 September 2005. There is some movement due to reworking of the sand waves and uncertainty in the surveys but there is no systematic movement of the sand waves indicating migration.

incorporates viscosity, grain size, water depth, and flow velocity. The relative roughness is flow depth over the grain size. Assuming the sand waves develop under rough flow

conditions, where the turbulence is not related to the grain size, the equation simplifies, and the wavelength remains dependant only on the flow depth. Yalin goes on to support his equations empirically. Yalin's prediction of sand wave height is based on shear stress, which implicitly includes viscosity, flow density, grain size, and flow velocity. The equation for height is also derived empirically from flume and river data.

Yalin's relationships are:

$$\eta = 0 \quad \tau < \tau_{cr} \quad \text{Equation 1}$$

$$\eta = \frac{h}{6} \left(1 - \frac{\tau_{cr}}{\tau} \right) \quad \tau_{cr} < \tau < 17.6\tau_{cr} \quad \text{Equation 2}$$

$$\eta = 0 \quad \tau \geq 17.6\tau_{cr} \quad \text{Equation 3}$$

$$\lambda = 2\pi h \quad \text{Equation 4}$$

where η is the sand wave height, τ is the shear stress, τ_{cr} is the critical shear stress, λ is the sand wave spacing, and h is the water depth. Van Rijn's sand wave height prediction also incorporates grain size, but his wavelength equation is still based only on water depth. Van Rijn's relationships are:

$$\eta = 0 \quad \tau < \tau_{cr} \quad \text{Equation 5}$$

$$\eta = 0.11h \left(\frac{d_{50}}{h} \right)^{0.3} (1 - e^{-0.5T_s}) (25 - T_s) \quad \tau_{cr} < \tau < 26\tau_{cr} \quad \text{Equation 6}$$

$$\eta = 0 \quad \tau \geq 26\tau_{cr} \quad \text{Equation 7}$$

$$\lambda = 7.3h \quad \text{Equation 8}$$

$$\text{where } T_s = \frac{\tau - \tau_{cr}}{\tau_{cr}} \quad \text{Equation 9}$$

and d_{50} is the median grain size. Both models predict no transport if the shear stress is less than the critical value, $\tau < \tau_{cr}$, and, therefore, no sand waves are predicted to develop if that condition is met. They also acknowledge a maximum shear stress beyond which bedforms are 'washed out.' Using values representative of the Moriches Inlet field site ($d_{50}=0.48$ mm and $h=3$ m) the height and length of the sand waves can be estimated. The shear stress was evaluated for a current velocity of 0.4 m/s, 0.5 m/s, and 0.6 m/s, and the associated shear stress values were 0.28 N/m², 0.43 N/m², and 0.62 N/m², respectively. The wavelength predictions are larger than observations, 19-22 m compared to an observed average wavelength of 15 m (Table 1). The standard deviation of the observed wave lengths is 4 m, so the prediction and observations agree. Sand wave height is consistently under-predicted, 2-29 cm compared to observations of 39 cm. The standard deviation of the sand wave heights measured at Moriches Inlet is 13 cm. Again, the predicted and observed values agree, albeit just barely.

Table 1. Predicted Sand Wave Heights and Wavelength

	$\bar{U} = 0.4$ m/s	$\bar{U} = 0.5$ m/s	$\bar{U} = 0.6$ m/s
Yalin Height (m)	0.04	0.20	0.29
Yalin Wavelength (m)		19	
van Rijn Height (m)	0.02	0.17	0.29
van Rijn Wavelength (m)		22	

\bar{U} is the depth-averaged velocity

MOBILIZATION OF THE SAND WAVE FIELD

The sand wave field at Moriches Inlet is a persistent feature which has been observed on aerial photographs from 2001 and 2004, and bathymetric surveys from 2004 and 2005, however, the conditions responsible for creating them was not observed during this study. Predictions of sand wave height based on flow velocity measured at Moriches Inlet (Yalin, Equation 2; van Rijn, Equation 6) under predict the height of the sand waves, suggesting that a stronger current velocity was responsible for building these features. Assuming these predictions are accurate, the flow conditions responsible for creating these features were likely not observed during this study.

Evidence for sand wave development under conditions different than those seen during this study is also evident in the slope of the slip face and the steepness of the sand waves. The sand waves display an asymmetrical profile, but the slip face is gently sloped and does not approach the angle of repose. This indicated that the sand waves are not actively migrating. These sand waves were likely actively migrating during their developing phase, but are now stationary because the net sediment transport is not sufficient to cause migration. The weak current and negligible sediment transport have modified the morphology of the sand waves but not erode them or reversed their orientation.

Given the reasons described above, it is concluded that the sand wave field at Moriches Inlet developed when flow conditions were stronger than those observed during this study, possibly during a storm surge or other meteorological event that increased the tidal current velocity. Since then, the typical flow conditions have gently reworked the sand waves, relocating the crests to a more central location, and flattening the slip face while the sand waves remain stationary.

The hypothetical event creating the sand waves can be reconstructed using the empirical equations for sand wave height published by van Rijn (1984) and Yalin (1964) and the physical relationship between tidal range and current speed. The observed sand wave height is 39 cm. To achieve this height, according to the relationships published by Yalin (1964) and van Rijn (1984), the current speed should reach 80 cm/s. Therefore, it can be assumed that the event creating these sand waves caused current velocity in the study area to increase to 80 cm/s.

The velocity of the tidal current is a function of the tidal prism. Because the tidal period remains constant, as the tidal prism increases, the water must flow faster in order to accommodate the larger flux. As long as the area of the bay is constant as the water level rises, tidal range is a valid proxy for tidal prism. In a bay with steep sides and few tidal flats, such as Moriches Bay, the area of the bay remains fairly constant throughout the tidal cycle and, therefore, the relation between tidal prism and current speed can be extrapolated to tidal range and current speed. The current data collected during this study also suggests the bay area remains constant as the water elevation nears high tide. The velocity gradually decreases near high tide; if there were large changes in the bay area as the tide rose, the velocity record would show an acceleration near high tide but it does not.

An increase in tidal range will increase the current speed. Changes in the tidal range are generally periodic and caused by lunar and solar forcing. However, there is also a stochastic component to the tides which is forced by metrological conditions such as wind and/or barometric pressure. For example, during a storm, low barometric pressure, wave setup, and wind forcing may increase or decrease the elevation of the water's surface. This change may increase the tidal range and, therefore, the current velocity.

The water level and current data collected at Moriches Inlet were used to calculate the tidal range and the peak current speeds so that a relationship between these two parameters could be defined. The linear regression between peak current speed and tidal range was calculated for four records. Other current records were disregarded because of the poor data quality (high signal-to-noise ratio or invalid velocities because the meter tipped over) or the length of the record (at least four days of measurements were needed). In addition to being a function of tidal prism, current velocity also depends on the bathymetry; therefore, the relationship between peak tidal current and tidal range is spatially dependent. Because of the spatial dependence, each record was analyzed separately (each record was collected from a slightly different location within the study area). These data were further separated by flow direction. In areas with an asymmetrical tidal signal, the relationship between the peak flood velocity and the tidal range is different than relation between the peak ebb velocity and the tidal range. The study area is generally flood-dominant, so the flood and ebb velocities were analyzed separately. The flood velocities were stronger and showed a better correlation to tidal range than did the ebb velocities. After the analysis was completed, one additional record was disregarded because it had a strong diurnal inequality which resulted in a poor correlation between the current velocity and the tidal range. The R-squared values for the individual stations were 0.73, 0.94, and 0.94. An overall relation between tide range and peak current velocity for the study area was obtained for these three stations (Figure 5):

$$U_{peak} = 0.12 + 0.41(\text{Tidal Range}) \quad \text{Equation 10}$$

where U_{peak} is the peak tidal current in m/s. For this equation, the R-squared value dropped to 0.51, but the inclusion of all the data makes it a more robust predictor for the

general study area. Based on the regression, the peak current velocity will be 80 cm/s when the tidal range is 1.66 m.

Water level data from Sandy Hook, NJ¹ and Shinnecock Bay² were used to evaluate the frequency of events with a tidal range exceeding 1.66 m. Shinnecock Inlet is 30 km east of Moriches Inlet, and the tide gauge was just inside the inlet (Figure 6). Sandy Hook is the National Oceanic and Atmospheric Administration (NOAA) reference station for Moriches Inlet. The correction for low water is 0.60, and the correction for high water is 0.62. These corrections were applied to the observed water levels measured at Sandy Hook to approximate the tidal range at Moriches Inlet (Figure 7). Between May 1998 and December 2005, the tidal range exceeded 1.66 m only once, on 12 December 2000. This tidal range could have increased the tidal velocity and created the sand wave field at Moriches Inlet. This large tidal range was caused by strong winds and a drop in atmospheric pressure. During that day, the wind velocity increased from 2 m/s to 19 m/s, and the wind turned from the north (Figure 8). In addition, the barometric pressure dropped below 1,000 pHa. The drop in atmospheric pressure raised the elevation of the high tide and wind amplified the ebb flow out of the bay and created an extra low low-tide. The result was an extremely large tidal range of 1.95 m.

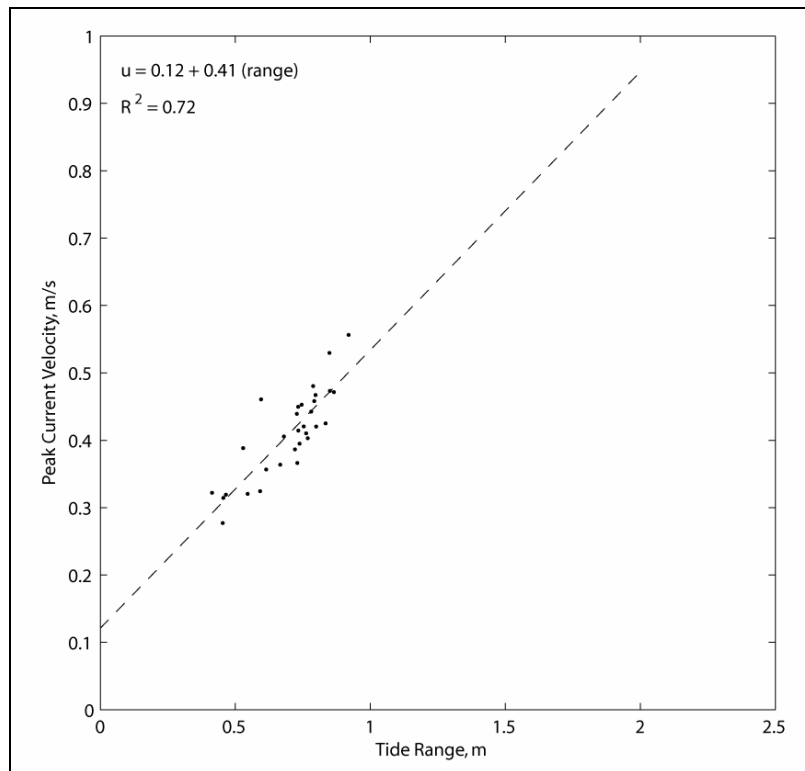


Figure 5. Generalize regression analysis for Moriches Inlet.

1 NOAA Tide Station 8531680 (40° 28.0' N, 74° 0.6' W)

2 The Shinnecock Bay tide gauge was maintained by the LIShore program under the direction of the USACE, Coastal Inlets Research Program.

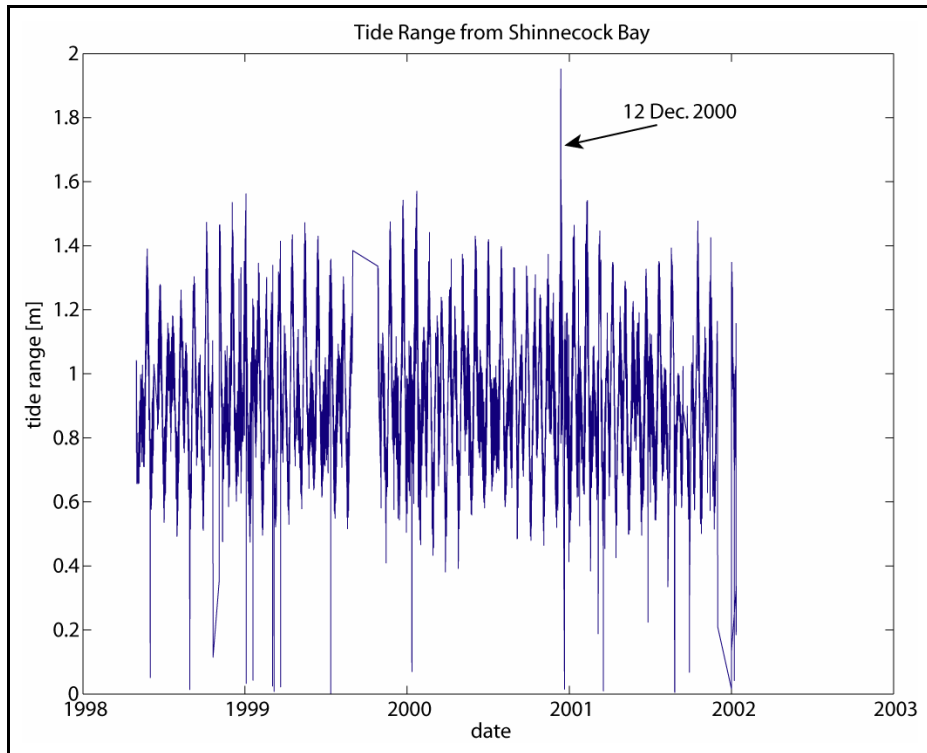


Figure 6. Tidal range at Shinnecock Inlet. Tidal range exceeds 1.66 m only on 12 December 2000, when it reached 1.95 m.

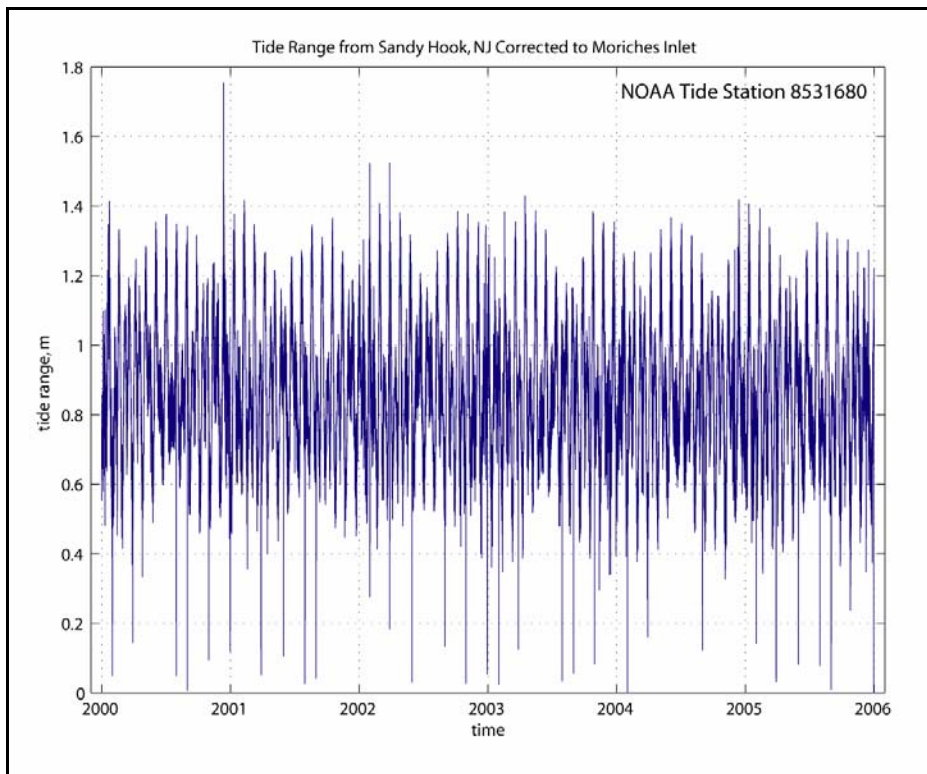


Figure 7. Tidal range at Moriches Inlet. Tidal range exceeds 1.66 m only on 12 December 2000.

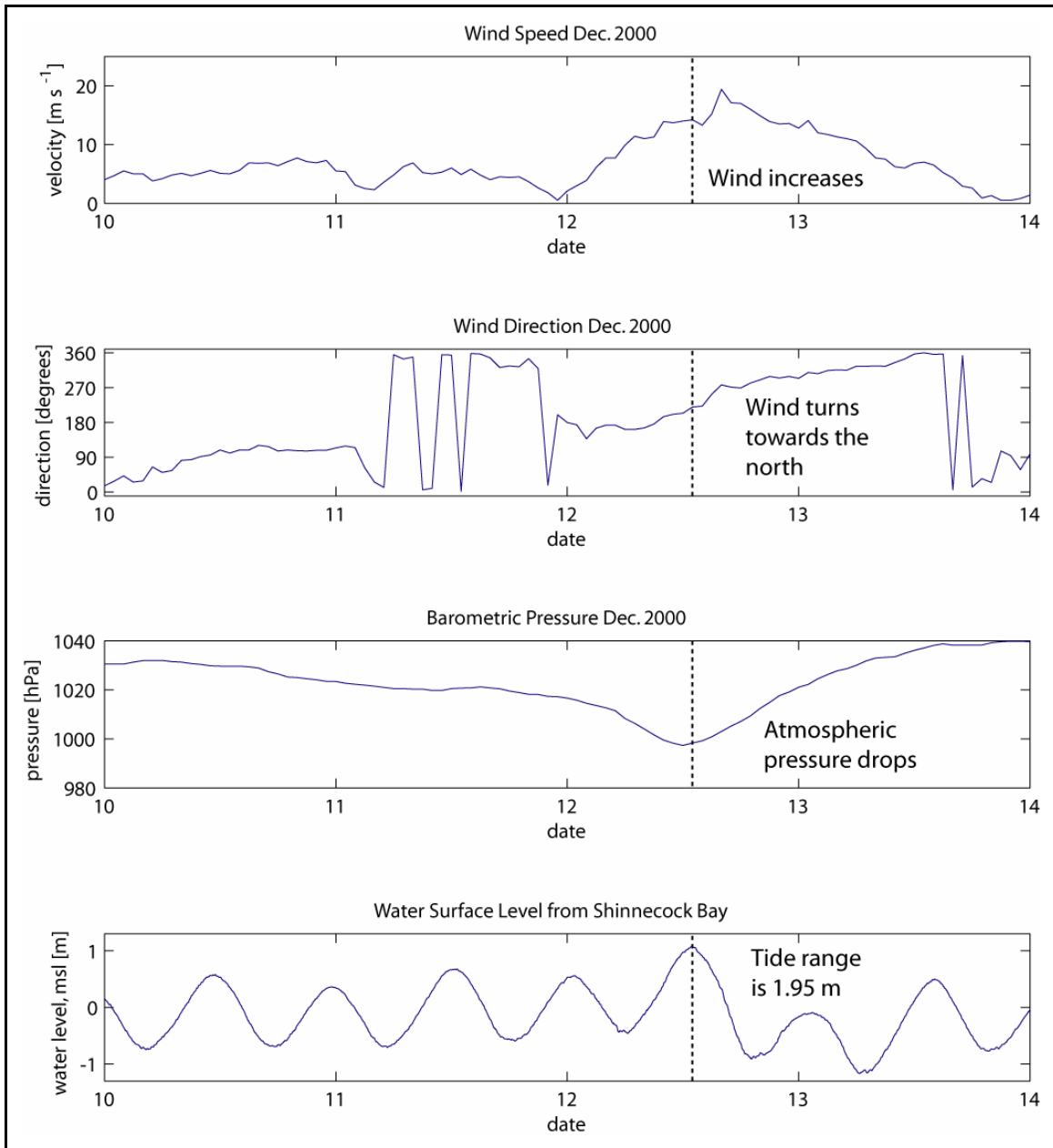


Figure 8. Wind speed and direction, barometric pressure, and water level at Shinnecock Inlet 10 December-14 December 2000. Wind data are from the National Data Buoy Center (Station 44025) and the water level data are from the LIShore Shinnecock Bay tide gauge.

CONCLUSION

The sand waves at Moriches were compared to predictive models of sand wave height presented by Yalin (1964) and van Rijn (1984). Both models are based on shear stress. Yalin's and van Rijn's equations under predicted the sand wave height by 10 cm. Their model both predict a sand wave height of 29 cm compared to 39 cm as measured at Moriches. Although the sand waves are asymmetrical, the slip face angle is very shallow. The average slope ranges from 3.8° to 4.7°. The steepest slip faces are 5.9°-6.2°.

It is unlikely that the observed flow conditions are responsible for the development of this sand wave field. According to Yalin's and van Rijn's predictions, the current velocities are too weak to build these features. Episodic storm events could increase the tidal currents, which could produce these features. After the passage of the storm the typical tidal currents continue to rework the sand waves. Slowly the sand wave crest is eroded and the slip face angle is flattened. Typical current conditions do not completely erode the sand wave but active migration is not observed during these conditions.

The observation of this moribund, or relic sand wave field at Moriches Inlet suggests that sand waves may persist long after the conditions responsible for their development have subsided. Once sand waves are present on the seabed, the bathymetric irregularities caused by these features help maintain the sand waves during extended periods of low flow conditions. During typical hydrodynamic conditions sand waves become autonomous or self maintaining. This conclusion suggests that infrequent high-energy flow events should be taken into account when trying to predict the development of sand waves.

ACKNOWLEDGEMENTS

The authors would like to thank the following organizations and individuals for their financial and technical support of this study:

- Office of Naval Research for graduate funding through the National Defense Sciences and Engineering Fellowship.
- Coastal Inlets Research Program, U.S. Army Corps of Engineers for their financial support of the field work.
- Geological Society of America for financial support of the field work through their Graduate Student Research Grant.
- Steven Borgeld, from Humboldt State University, for supplying the grain size data for the Humboldt Entrance Channel.

REFERENCES

- Aliotta, S. and Perillo, G. M. E. (1987). "A sand wave field in the entrance to Bahia Blanca estuary, Argentina," *Marine Geology* 76, 1-14.
- Boothroyd, J. C. and Hubbard, D. K. (1975), "Genesis of bedforms in mesotidal estuaries," in L. E. Cronin, ed., *Estuarine Research*, Vol. II: New York, New York, Academic Press, Inc., p. 217-234.
- Dalrymple, R. W., Knight, J. R. and Lambiase, J. J. (1978). "Bedforms and their hydraulic stability relationships in a tidal environment, Bay of Fundy, Canada," *Nature* 275, 100-104.
- Dalrymple, R. W. and Rhodes, R. N. (1995), "Estuarine dunes and barforms," in G. M. E. Perillo, ed., *Geomorphology and Sedimentology of Estuaries*, Elsevier Science, p. 359-422.
- Gabel, S. L. (1993). "Geometry and kinematics of dunes during steady and unsteady flows in the Calamus River, Nebraska, U.S.A.," *Sedimentology* 40, 237-269.
- Mazumder, R. (2003). "Sediment transport, aqueous bedform stability and morphodynamics under unidirectional current: a brief overview," *Journal of*

- African Earth Sciences* 36, 1-14.
- McCave, I. N. (1971). "Sand waves in the North Sea off the coast of Holland," *Marine Geology* 10, 199-125.
- Southard, J. B. (1971). "Presentation of bed configurations in depth-velocity-size diagrams," *Journal of Sedimentary Petrology* 41(4), 903-915.
- Southard, J. B. and Boguchwal, L. A. (1990). "Bedform configurations in steady unidirectional water flows. Part 2: synthesis of flume data," *Journal of Sedimentary Petrology* 60(5), 658-679.
- van Rijn, L. C. (1984). "Sediment transport, part III: bed forms and alluvial roughness," *Journal of Hydraulic Engineering* 110(12), 1733-1754.
- Yalin, S. M. (1964). "Geometric properties of sand waves," *Journal of the Hydraulics Division* 90(HY5), 105-120.
- Zarillo, G. A. (1982). "Stability of bedforms in a tidal environment," *Marine Geology* 48, 337-351.